Pure & Appl. Chem., Vol. 67, No. 1, pp. 1–8, 1995.
Printed in Great Britain.

What can electron impact spectroscopy offer to photochemistry? Triplet states, negative ions and intramolecular electron transfer

Michael Allan

Institut de Chimie Physique de l'Université, Pérolles, CH-1700 Fribourg, Switzerland

Abstract: The principles of the electron impact methods Electron Energy Loss (EEL) spectroscopy, Electron Transmission (ET) spectroscopy, measurement of Energy-Dependence (ED) of vibrational excitation, and Dissociative Attachment (DA) spectroscopy are briefly introduced. The possibilities of modern instrumentation are illustrated with the examples of molecular oxygen and 1,3-butadiene. The following subjects of current interest are then discussed: (i) Triplet states and electron affinities of saturated hydrocarbons, including aliphatic hydrocarbons and compounds with increasing degree of strain, cyclopropane and (1.1.1)propellane. (ii) Dissociative attachment experiments on dihalosubstitued toluenes providing insight into factors determining the rate of intramolecular charge-transfer in the gas phase.

1. INTRODUCTION

Electron Impact (EI) Spectroscopy has early beginnings, it started with the crude electron-energy-loss (EEL) experiments of Franck and Hertz in 1914, and continued with the first measurements of electron-atom and electron-molecule collision cross sections in the 1930's. Important impetus to electron collision research was given by the discovery of short-lived negative ions (also called resonances) in electron-molecule collisions in the 1960's and 1970's and the accompanying development of high-resolution instrumentation (1). The research in this time period concentrated on atoms, diatomic and triatomic molecules.

First applications to chemistry can be traced to the early 70's and evolved along two main lines:

- Electron-Energy-Loss-Spectroscopy (EELS) was used to observe spin and dipole forbidden transitions in organic compounds. The pioneering work of Kuppermann (2) can be taken as a representative example.
- Electron Transmission Spectroscopy (ETS) was used to study temporary negative ions of organic compounds, with the aim to assess the electron affinities, the properties of virtual orbitals, and electronic structure of negative ions. Much of the pioneering work has been initiated by Burrow and Jordan (3).

The results of the early experiments proved very useful for chemistry and a pursuit of this direction of research was therefore initiated in Fribourg in 1981.

The capability of the EI techniques to give information on excited states and on virtual orbitals makes it an interesting support tool for photochemistry. The techniques are, despite the early beginnings, still in the stage of active development, comprising both further development of the gas phase instrumentation, improving the quality and reliability of the results and facilitating simpler application to a wider range of compounds, and extending the applications to molecules adsorbed on surfaces and molecules imbedded in low temperature matrices (4).

2. INSTRUMENTAL SECTION

This section describes the instrumentation used in Fribourg.

2.1. Trochoidal electron spectrometer

This instrument, described in detail in ref. (5), uses an axial magnetic field to focus the electron beam. It is capable of recording ET-spectra, EEL-spectra, and excitation functions for specific vibrational and electronic excitation processes, albeit at a fixed scattering angle. It offers specific advantages over "traditional" electrostatic instruments in terms of very high sensitivity, low sample consumption (useful spectra can be obtained with 50 mg of sample), and sustained performance at very low electron energies. With a high temperature attachment, it can also measure low-volatility compounds like fullerene C_{60} (6).

2.2. Dissociative electron attachment spectrometer

This recently improved (7) instrument, described for example in ref. (8), studies dissociative decay channels of the temporary anions. The instrument also uses a magnetically focused trochoidal electron monochromator to prepare a quasi-monoenergetic beam of electrons, incorporates an electrostatic analyser for measurement of the fragment anion kinetic energies, and a quadrupole mass filter for fragment mass analysis.

2.3. Electrostatic electron spectrometer

This is the most recently constructed instrument and is described briefly in ref. (9). It permits recording signal as a function of scattering angle and offers higher resolution (up to 12 meV, depending on sensitivity) than the trochoidal instrument. In its most recent version, it permits recording of absolute differential cross sections (10, 11). It is an essentially standard electrostatic spectrometer using hemispherical deflectors for electron energy selection, but careful choice of materials (molybdenum for optics, mostly titanium for structural elements), consequent computer control (64 digital-to-analog converters generate the focusing and deflecting voltages), and other technical details result in improved performance. This instrument does, however, use much more sample, about 10 g are required for an average study.

3. APPLICATIONS

3.1. Electron-Energy-Loss Spectroscopy

This techniques may be used to determine excitation energies for molecules of photochemical interest, in particular where the transition from the ground state is spin or dipole forbidden.

This chapter starts with the examples of oxygen and butadiene, illustrating the power of modern instrumentation. Fig. 1 shows an energy-loss spectrum of oxygen, recorded with the electrostatic spectrometer in Fribourg. It shows the "singlet oxygen" state very clearly and could be useful in textbooks to visualize this important species.

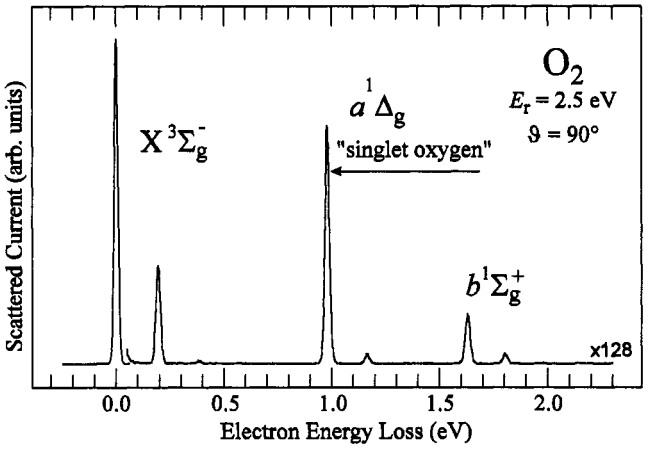

Fig. 1 EEL spectrum of oxygen.

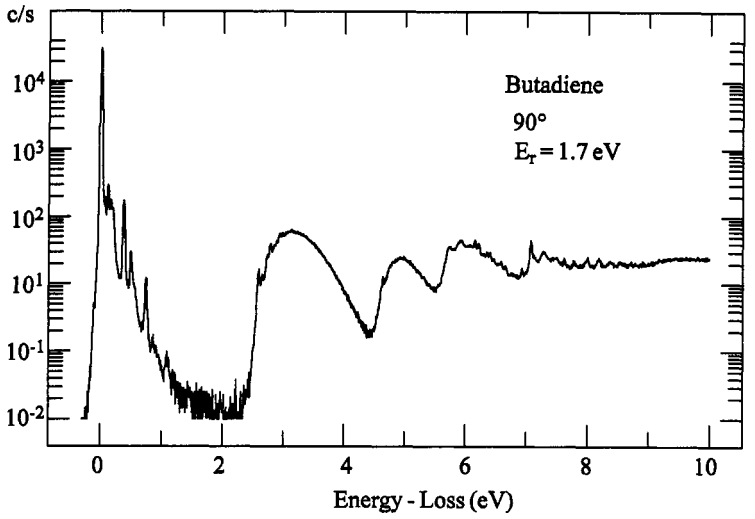

Fig. 2 Global EEL spectrum of 1,3-butadiene.

Fig. 2 shows an energy-loss spectrum of butadiene, also recorded with the electrostatic spectrometer in Fribourg. It agrees well with the earlier spectrum of Kuppermann (12), but illustrates clearly the improvements in instrumentation. The spectrum is shown on a semilog scale to accommodate the large dynamic range of the signals. It shows the elastic peak at $\Delta E = 0$, followed by peaks due to vibrational excitation. Bands due to triplet and singlet excited states can be discerned at higher energy losses. Noteworthy is the large dynamic range covered by the instrument: there are six orders of magnitude between the background level and the height of the elastic peak, even the relatively weak electronic excitation is a factor of hundred above the background. Furthermore, the computer control permits non-linear adjustments of the beam focusing voltages and thus scans over large energy ranges, yielding global views of the electronic structure of a given molecule. The resolution (about 25 meV in combination with the sensitivity of Fig. 2) permits observation of vibrational structure as exemplified by the detail of the T_1-band in Fig. 3. The observed excitation of the C=C and C-C stretch and C-C-C deformation vibrations is in line with the bonding and antibonding nature of the well known π and π^* orbitals involved in this transition. Interesting is the similarity with the vibrational structure brought about by a temporary occupation of the π^* orbital, shown in Fig. 5, Sec. 3.2.

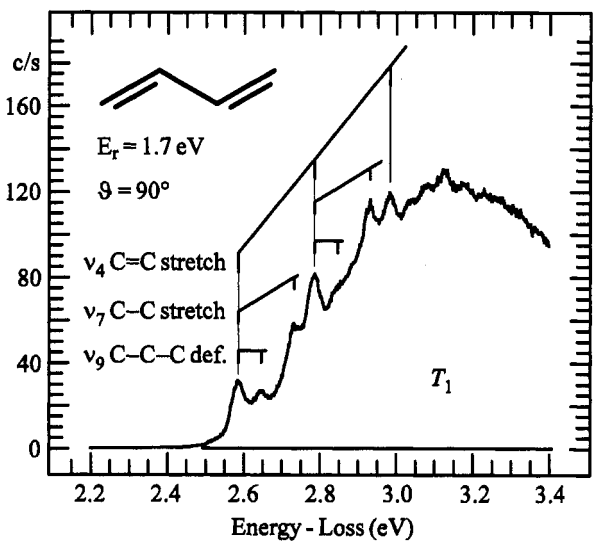

Fig. 3 Detail of the T_1 band of butadiene.

The power of the EEL-spectroscopy to show the global view of the excited state of a given molecule is very useful in visualizing the trends in the electronic structure of a series of molecules. This is exemplified in Fig. 4, showing the EEL-spectra of three hydrocarbons.

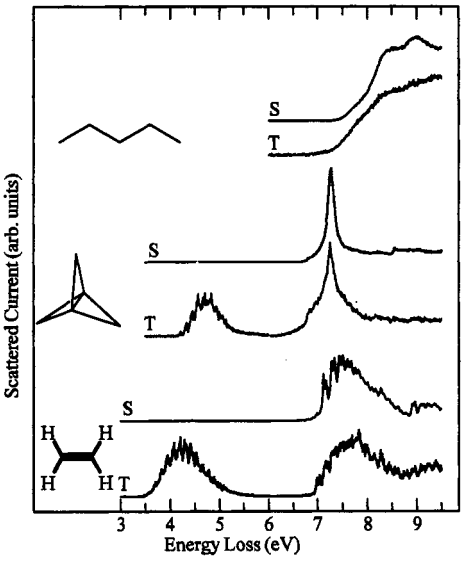

Fig. 4 Comparison of EEL spectra of *n*-pentane, (1.1.1) propellane, and ethene. The ethene spectra were recorded with the electrostatic spectrometer, the remaining spectra with the trochoidal spectrometer. The spectra labelled S are recorded under "singlet conditions", that is with high residual energy and/or low scattering angle and show the dipole allowed transitions. The spectra labelled T are recorded under "triplet conditions", that is with low residual energy and/or large scattering angle and show both the dipole allowed and dipole/spin forbidden transitions.

The spectrum of *n*-pentane (13) is representative for saturated aliphatic hydrocarbons. The lowest excitation energies are very high. The onsets of the signals under triplet and singlet conditions are similar, indicating very small singlet-triplet splitting, and thus Rydberg nature of even the lowest excited states (14). The bands are broad and structureless, resembling the UV-photoelectron bands, in line with the Rydberg assignment. This type of spectra is given by the low-lying HOMO and high-lying valence unoccupied orbitals in aliphatic hydrocarbons.

The stretched central bond in [1.1.1]propellane is associated with a relatively high-lying HOMO and low-lying valence LUMO. This is born out in the spectrum (15), with a low-lying triplet state and a large singlet-triplet splitting. The relation between low-lying $\sigma \rightarrow \sigma^*$ triplet and low homolytic dissociation energy described by Michl (16) is borne out. The effect of the bridge bond on electronic structure is so dramatic that it makes the spectrum of propellane resemble the spectrum of ethene, shown for comparison in the lower part of Fig. 4 (see ref. (13) for a discussion of the ethene spectrum, ref. (11) for the present spectrum).

Interesting is the comparison of band widths of ethene and propellane. The valence triplet states are of comparable widths, a fact which could be explained by comparable bonding and antibonding character of the HOMO and LUMO orbitals in the two compounds. The valence singlet bands, however, have dramatically different width in the two compounds: the S_1 band in ethene (it is partially obscured by sharp Rydberg transitions, but the width is well discernible) is wide, comparable to the T_1 band, the S_1 band of propellane is unusually narrow. This fact could in part be due to the excitation of twisting vibration in ethene (the S_1 state equilibrium geometry is perpendicular), but a full explanation deserves further study.

3.2 The study of resonances

The states of the butadiene negative ion, corresponding to temporary occupation of the virtual molecular orbitals, were determined to lie at 0.62 eV (π_1^* LUMO) and 2.8 eV (π_2^*) by ET spectroscopy (17). Such states are short-lived due to autodetachment, and are interchangeably called short-lived negative ion states,

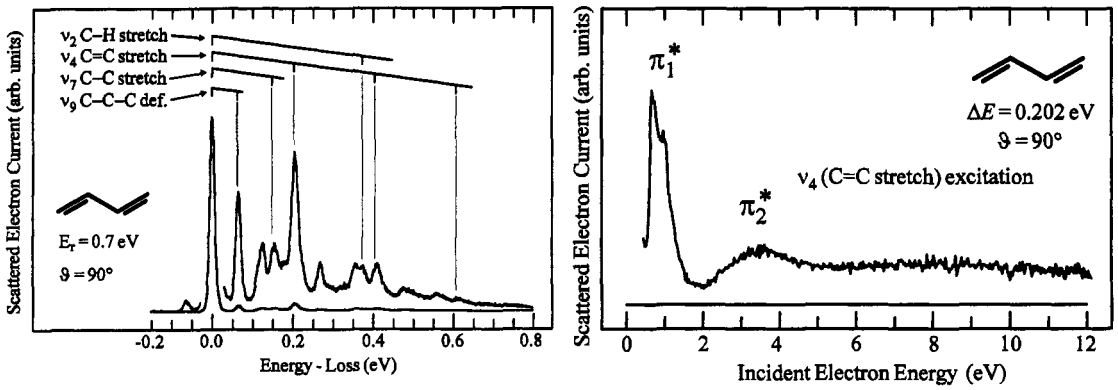

Fig. 5 Left: EEL spectrum of butadiene showing vibrational excitation caused by the π_1^* resonance, that is by the temporary occupation of the π_1^* LUMO. The resolution is 12 meV. Right: Excitation function of the C-C stretching vibration in butadiene, showing peaks due to the π_1^* and π_1^* resonances.

resonances or negative ion resonances. The lifetime of the short-lived anion formed by the attachment of an incident electron to the target molecule in resonant scattering is often of the same order of magnitude as the vibrational period. The nuclei of the target molecule thus relax on the anion potential surface for a short time, causing vibrational excitation of the target molecule after the anion has eventually decayed back to the neutral molecule through autodetachment. Which vibrations have been excited is thus informative of the nature of the distortion which the molecular skeleton experienced during the lifetime of the negative ion.

Symmetry rules and a very specific distortion caused by distinct antibonding properties of the temporarily occupied orbital generally cause the excitation of only very few vibrations even in polyatomic molecules with many vibrational modes, as has been shown in the pioneering studies on benzene (18) and ethene (19). This effect is illustrated here on the vibrational excitation of 1,3-butadiene caused by temporary occupation of the π_1^* MO, shown in Fig. 5. Only few of the 24 vibrational modes (20) are excited. The dominant vibration is C=C stretch, excited by the prolongation of the C=C bond by the temporary occupation of the π_1^* MO. Excitation of a C-C-C deformation vibration is second in intensity, indicating substantial changes of the C-C-C angle in the negative ion. The vibrational excitation spectra are thus very useful for characterizing the nature of the temporarily occupied MO, and for assigning resonances.

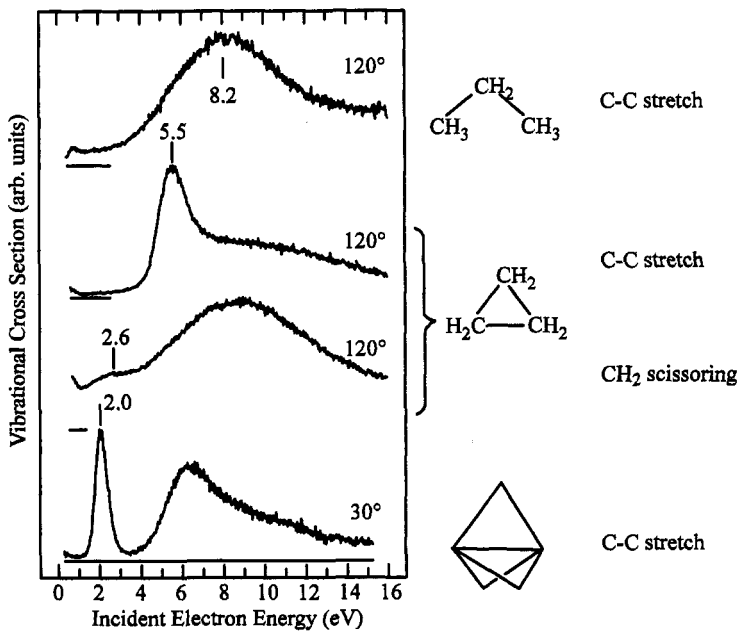

Fig. 6 Excitation functions of selected vibrations for three saturated hydrocarbons.

The fact that resonances strongly enhance vibrational excitation can be used to detect them by recording the dependence of exciting some given vibration on incident energy (energy-dependence, ED, spectrum), as shown for the excitation of the C=C stretch vibration in butadiene in Fig. 5. The spectrum clearly shows the π_1^* and π_2^* resonances, and very broad σ^* resonances at higher energies.

This method of determining resonant energies has an advantage over the ET spectroscopy in particular for broad resonances, which cannot be discerned clearly in the ET spectra. This advantage is exploited in Fig. 6 to study the often very broad σ^* resonances in saturated hydrocarbons. The top curve shows excitation function of a C-C stretch vibration of *n*-propane. One extremely broad band is observed, with an onset at about 3 eV, and a maximum around 8 eV. This result indicates one or more (overlapping) broad σ^* resonances at relatively high energies and low affinity towards electrons, in line with general chemical experience. Note that ET spectroscopy does not give any resonant bands in the linear saturated hydrocarbons, an example of *n*-pentane was given in ref. (15). The shape of the excitation function varies little with the length of the chain, nearly identical curve was obtained for ethane (21) and is representative of any linear saturated hydrocarbon.

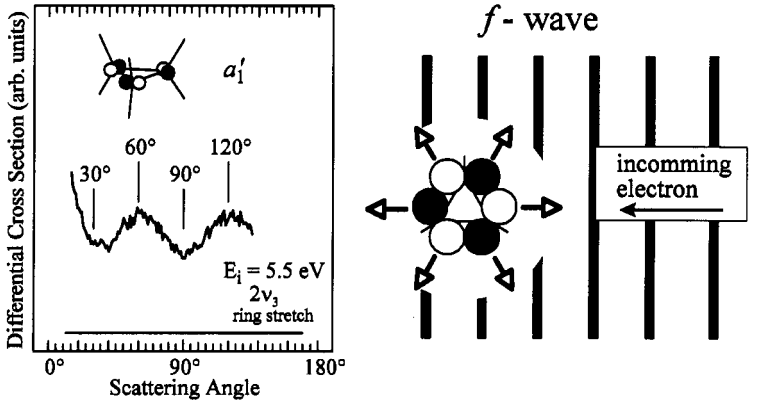

Fig. 7 Left: Angular distribution of electrons having excited two quanta of the symm. ring stretch vibration of cyclopropane *via* the 5.5 eV resonance. Observe the maxima in the forward direction, at 60° and at 120°. Right: Qualitative explanation of the angular distribution. The heavy vertical bars signify ridges of the incoming electron's plane wave. The a_1' MO, temporarily occupied in the resonance, is shown schematically in the orientation optimal for electron capture. Short bold arrows indicate preferred directions of the departing electrons.

On the other hand the additional strain in cyclopropane has a dramatic effect on the excitation functions (22). A band peaking at 2.6 e is observed in the excitation function of the CH_2 scissoring vibration, indicating a sizeable increase of affinity towards electrons. Secondly, a resonance is observed at 5.5 eV in the excitation function of the symmetric C-C stretch vibration, which is unusually narrow for its high energy. The observed angular distribution, shown in Fig. 7, allows the assignment of this resonance to temporary occupation of a a_1' MO, revising the original assignment of this band in the ET spectrum.

Finally, the lowest curve of Fig. 6 illustrates the dramatic effect which the stretched bridge bond has on the σ^* energy in [1.1.1]propellane.

3.3 Dissociative attachment

Dissociative electron transfer in solution

$$RX + e^- \rightleftharpoons R^{\cdot} + X^-,$$

where $R^{\cdot}$ is a carbon-centered radical, X is a halogen, and an electron is taken from an electrode or a suitable donor, is an extensively studied process because of its technological and ecological relevance. This work is concerned with the gas-phase counterpart of this process, the dissociative electron attachment (DA),

$$RX + e^- \rightarrow [RX^-] \rightarrow R^{\cdot} + X^-.$$

where a free electron is captured by an isolated molecule to form a short-lived negative ion $[RX^-]$ which may then dissociate into a stable X^- and a radical $R^{\cdot}$.

We study the *intramolecular* competition of two dissociation processes in the dihalogen compounds **1-6**, carrying simultaneously a halogen connected directly to the benzene ring (phenylic C-X bond) and the other separated by a methylene group (benzylic C-X bond) (23).

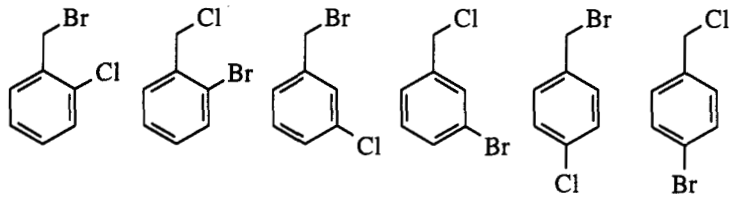

1 **2** **3** **4** **5** **6**

The experiment shows that an attachment of slow electrons (0-0.8 eV) results in X^- production for all above compounds. Mass spectra recorded at incident energies within this low energy DA-band (example is shown in Fig. 8) show that the signal of the benzylic X^- is approximately tenfold higher than the yield of phenylic X^- for all substitution patterns and irrespective of whether X is Cl or Br.

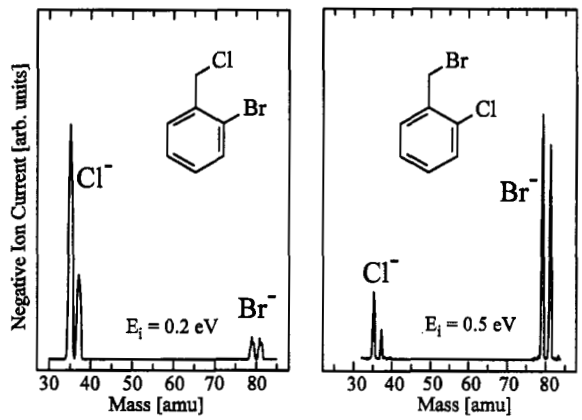

Fig. 8 Negative ion Mass spectra obtained with incident electron energies indicated, for **1** and **2**.

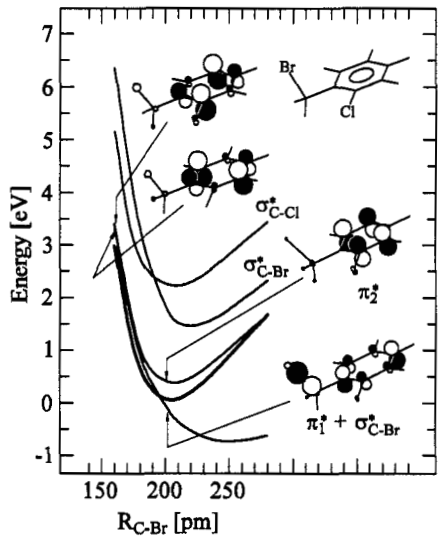

Fig. 9 Potential energy of the compound **1** (bold line) and its radical anion (thin lines) in function of the C-Cl distance, obtained from a HF/LANL1DZ calculation with application of Koopmans' theorem. (23) Schematic diagrams of the singly occupied orbitals were drawn using the program MOPLOT.(24) Arrows point to the potential curve and the internuclear distance to which the orbital diagrams apply.

This observation is interpreted as a result of both energy and symmetry effects. The loss of benzylic X^- is, on the one hand, favored energetically as a result of the weaker benzylic C-X bond. On the other hand the effect of symmetry appears to be important, because the selectivity of the dissociation remains preserved even when Cl and Br are interchanged, that is even when the energetics is substantially changed.

The symmetry argument is based on the fact that the molecules **1-6** may be approximately viewed as possessing a local plane of symmetry in the benzene ring. The phenylic halogen is lying in this plane, the intramolecular electron transfer from the π^* into the corresponding σ^* orbital and the ensuing DA are symmetry forbidden. The benzylic C-X bond is rotated out of the local symmetry plane for steric reasons, permitting efficient π^*/σ^* coupling, intramolecular electron transfer and dissociation. This situation is illustrated by the potential curves and orbital diagrams in Fig. 9. It shows that the $\sigma^*_{C\text{-}Cl}$ does not appreciably mix with the π^* MO's of the benzene ring, but the mixing of $\sigma^*_{C\text{-}Br}$ and π^* is substantial, resulting in a dissociative potential curve. Fig. 9 also illustrates the intramolecular electron transfer by showing that the lowest MO of the anion is essentially a benzene π^* at low C-Br distances, but becomes progressively a $\sigma^*_{C\text{-}Br}$ MO as $R_{C\text{-}Br}$ is increased.

REFERENCES

1. G. J. Schulz. *Rev. Mod. Phys.* **45**, 423 (1973).
2. A. Kupperman, W M. Flicker and O. A. Mosher. *Chem. Rev.* **79**, 77 (1979).
3. K. D. Jordan and P. D. Burrow. *Chem. Rev.* **87**, 557 (1987).
4. P. Swiderek, M.-J. Fraser, M. Michaud and L. Sanche, *J. Chem. Phys.* **100**, 70 (1994); D. Antic, D. E. David and J. Michl, posters at this conference; R. Azria, Y. LeCoat, J.-P. Ziesel, J.-P. Guillotin, B. Mharzi and M. Tronc, *Chem. Phys. Lett.* **220**, 417 (1994); M. Meinke and E. Illenberger, submitted to *J. Chem. Phys.* (1994).
5. M. Allan. *J. Electr. Spectr.* **48**, 219 (1989).
6. Ch. Bulliard, M. Allan, S. Leach. *Chem. Phys. Lett.* **209**, 434 (1993).
7. C. Bulliard, Ph.D. thesis, Fribourg 1994.
8. Y. Pariat, M. Allan. *Int. J. Mass Spectr. Ion Proc.* 103, 181 (1991).
9. M. Allan. *J. Phys. B: At. Mol. Opt. Phys.* 25, 1559 (1992).
10. M. Allan. *J. Chem. Phys.*, in print.
11. M. Allan. *Chem. Phys. Lett.*, in print.
12. O. A. Mosher, W. M.. Flicker and A. Kuppermann. *Chem. Phys. Lett.* 19, 332 (1973).
13. K. Asmis, S. El houar and M. Allan, unpublished.
14. M. B. Robin, *Higher Excited States of Polyatomic Molecules*, Vol. III, Academic Press, Orlando (1985).
15. O. Schafer, M. Allan, G. Szeimies and M. Sanktjohanser. *J. Am. Chem. Soc.* 114, 8180 (1992).
16. J. Michl. *Acc. Chem. Res.* 23, 127 (1990).
17. K. D. Jordan and P. D. Burrow, *Acc. Chem. Res.* 11, 341 (1978).
18. S. F. Wong and G. J. Schulz. *Phys. Rev. Lett.* 35, 1429 (1975).
19. I. C. Walker, A. Stamatovic and S. F. Wong. *J. Chem. Phys.* **69**, 5532 (1978).
20. T. Shimanouchi. *Tables of Molecular Vibrational Frequencies*, Consolidated Volume I, National Standard Reference Data Series 39; U.S. National Bureau of Standards; U.S. Government Printing Office: Washington, DC, 1972.
21. L. Boesten, H. Tanaka, M. Kubos, H. Sato, M. Kimura, M. A. Dillon and D. Spence. *J. Phys. B* 23, 1905 (1990).
22. M. Allan. *J. Am. Chem. Soc.* 115, 6418 (1993).
23. C. Bulliard, M. Allan and E. Haselbach, submitted to *J. Phys. Chem.* (1994).
24. A. Schmelzer and E. Haselbach, *Helv. Chim. Acta* 54, 1299 (1971). Improved and modernized version of T. Bally, B. Albrecht and S. Matzinger.